Astron. Astrophys. 336, 301–308 (1998)

ASTRONOMY
AND
ASTROPHYSICS

Diffuse radiation in models of photoionized nebulae

S.R. Och[1], **L.B. Lucy**[2], **and M.R. Rosa**[2,⋆]

[1] Dr. Remeis-Sternwarte, Astronomisches Institut der Universität Erlangen-Nürnberg, Sternwartstrasse 7, D-96049 Bamberg, Germany,
[2] Space Telescope-European Coordinating Facility, European Southern Observatory, Karl-Schwarzschild-Strasse 2, D-85748 Garching, Germany (llucy@eso.org)

Received 20 December 1996 / Accepted 19 December 1997

Abstract. This paper is the first in a series from a study of inhomogeneous gaseous nebulae, which has at its focus the apparent discrepancy between various observational aspects of real H II regions and theoretical predictions such as emission line ratios from low and high ionization species, details of the temperature structure and chemical abundance determination schemes. It is shown that the key problem is the detailed treatment of the radiation transport in an inhomogeneous and non-isotropic medium. We use a Monte Carlo technique, a proven means to handle complex radiation transport situations, to create photoionization models which are free of approximations concerning the radiative transfer. The code is tested for 1D homogeneous cases against the results from established photoionization codes, reaffirming its applicability to highly structured and non-symmetric nebulae.

Key words: ISM: H II regions – radiative transfer – atomic processes – methods: numerical

1. Introduction

Strömgren in 1939 was the first to provide a consistent theory of H II regions, predicting the ionization structure observed in gaseous nebulae from principles of atomic physics. Since then appreciable effort has been put into the development of photoionization models (for a recent review see Ferland et al. 1995). In spite of the simplifications necessary to analytically treat the radiation transport (1D geometry, homogeneity, isotropy), such models are capable to predict to a large degree integral properties of classical H II regions.

Continual improvement of photoionization modeling is crucial, since such models are, one way or the other, required to derive accurate elemental abundances from observed line fluxes. Either one compares the observed spectrum directly with sequences of models (eg. Garnett, 1990), or one obtains the correction factors for unobserved stages of ionization from models (eg. Mathis & Rosa, 1991). Also, photoionization modeling provides a guide as to which of the observed electron temperatures one should use in order to convert emissivities of collisionally excited transitions into particle numbers. Ultimately the chemical composition of the ionized interstellar medium so derived from observations of H II regions is at the basis of our ideas about stellar and galactic evolution, and of the universe as a whole.

However, discrepancies become apparent when model ionization structures and line emissivities are compared to detailed observations of real nebulae. In particular, the emission line ratios between low and highly ionized species are generally underestimated by models (see discussion by Mathis, 1976). Similarly, observations at different positions in the same nebula cannot successfully be explained by a single homogeneous model, even if the ionization parameter U (e.g. Mathis, 1985), defined as the ratio of photon- to electron density, is varied. While the high ionization regimes are in general reproduced very well, the predominantly low-ionization regions do not fit the computed tracks in diagnostic diagrams, even when taking into account a composite model with more than one effective temperature for the ionizing radiation (Mathis, 1982, 1985; Mathis & Rosa, 1991).

Having in mind the filaments and knots seen in every spatially resolved nebula, e.g. the HST image of Orion (cf. Hester et al., 1991), it is worth reconsidering the common model assumptions on symmetries and homogeneity. Blobs of enhanced density not only modify the local emissivities but have an effect on the nebular condition in the surrounding material as well through modification of the ambient diffuse radiation field. Opaque blobs give rise to regions protected from direct starlight, building up extended shadow zones (see e.g. Mathis, 1995). In such regions the ionization is maintained by the diffuse radiation originating from outside. Since the diffuse ionizing radiation often is softer than the stellar component one expects enhancements of low ionization species with respect to the unobstracted environment. Such regions might contribute to the spatially integrated nebular emission in a way which would account for the above mentioned discrepancies between observations and model line intensity ratios. However, photoionization models of more realistic nebulae including inhomogeneities have to properly solve the radiative transfer. Even for rather simple semi-homogeneous cases this turns out to be a formidable task in analytic codes.

Send offprint requests to: Michael R. Rosa

⋆ Affiliated to the Astrophysics Division of the Space Science Department of the European Space Agency (mrosa@eso.org)

In view of this a numerical technique is sought which can handle the radiation transport adequately without the need to impose symmetries, i.e. for arbitrary density distributions and geometries. A rather similar problem exists in expanding stellar winds around hot stars where the line radiation transport happens in a strong velocity field. The latter case was successfully modeled by Abbott & Lucy (1985) and Lucy & Abbott (1993), who developed a Monte Carlo method to derive the radiation field in a straightforward manner. This approach of treating the radiation transport in non-homogeneous media by Monte Carlo techniques offers a natural solution for the simulation of a gaseous nebula. In the present paper we develop the technique and demonstrate its successful application to a homogeneous case by comparing the results with conventional photoionization models, in order to provide the basis for its application to generalized density distributions.

In Section 2 we discuss the radiation transport problems in complex nebulae. Then, in Sect. 3, a Monte Carlo technique is presented, which is independent of the chosen density structure and treats the radiation field as well as the ionization and the energy equilibria in a self-consistent manner. A complete description of the nebular simulation is given in the fourth section. In Sect. 5 the results of the Monte Carlo model for the homogeneous case are compared with standard several photoionization models. Finally, we outline extensions to realistic model nebulae.

2. Nature of the radiation field

In order to derive the physical conditions (ionization state, T_e) of a nebula from the principle of detailed balancing, the rates of all radiative and collisional processes have to be computed. Therefore the radiation field at any location in the ionized volume needs to be determined. At first a finite volume element $\mathrm{d}V$ at a position $\boldsymbol{x}$ in the nebula is exposed to photons emerging from the ionizing star. These photons have a unique, well-defined direction when arriving in $\mathrm{d}V$, namely pointing away from the star towards $\mathrm{d}V$ (for the moment the extension of the source is neglected). When traversing the nebular gas, the stellar radiation suffers from absorption which is characterized by the optical depth $\tau_\nu(\boldsymbol{x})$. Further the radiation is attenuated due to geometric dilution, given by $W(\boldsymbol{x})$. Together this results in a mean stellar intensity at position $\boldsymbol{x}$ in the nebula of

$$4\pi J_\nu^{\mathrm{st}}(\boldsymbol{x}) = \pi F_\nu^* W(\boldsymbol{x}) e^{-\tau_\nu(\boldsymbol{x})} \quad (1)$$

where πF_ν^* is the flux emitted by the stellar source.

Secondly, in addition to the stellar part, the gas itself emits radiation as a consequence of recombination of ions with free electrons. The corresponding volume emissivity of this diffuse (isotropical) radiation can be expressed by applying the Milne relation:

$$j_\nu = \frac{2\mathrm{h}\nu^3}{\mathrm{c}^2}\frac{\omega_i}{\omega_{i+1}}\left(\frac{\mathrm{h}^2}{2\pi\mathrm{m}\mathrm{k}T_\mathrm{e}}\right)^{2/3} a_\nu(X_i) e^{-\mathrm{h}(\nu-\nu_o)/\mathrm{k}T_\mathrm{e}} X_i N_\mathrm{e} \quad (2)$$

where ω_i and ω_{i+1} stand for the ground state statistical weights of the ions involved, X_i for the abundance of the recombining ion, $a_\nu(X_i)$ for the photoionization cross section, and ν_o for the ionization threshold. Since the sources of diffuse radiation are distributed all over the nebula, any other volume element $\mathrm{d}V'$ contributes to the diffuse radiation field at $\boldsymbol{x}$ in $\mathrm{d}V$. Photons arriving from differing regions are attenuated by geometric dilution and absorption analogous to the stellar component. However, although the diffuse photons are emitted isotropically, the absorption is different for various directions in the nebula which destroys the isotropy. The mean diffuse intensity can be written as the integral over the source function $\frac{j_\nu}{\kappa_\nu}$, where $\kappa_\nu(\boldsymbol{x})$ denotes the opacity, radiation originating from all optical depths and covering the full solid angle:

$$J_\nu^{\mathrm{dif}}(\boldsymbol{x}) = \int_\Omega \int_{\tau_\nu}^{\infty} \frac{j_\nu}{\kappa_\nu} \mathrm{e}^{-(t-\tau_\nu)} \mathrm{d}t\, \mathrm{d}\omega. \quad (3)$$

The mean intensity is derived from the specific intensity I_ν appearing in direction $\boldsymbol{n}$ by summing over the complete solid angle. The problem then consists in the calculation of the processed I_ν at position $\boldsymbol{x}$. This is generally done by solving the radiation transport equation for I_ν given by:

$$(\boldsymbol{n}\cdot\frac{\mathrm{d}}{\mathrm{d}\boldsymbol{x}})\, I_\nu(\boldsymbol{x},\boldsymbol{n}) = -\kappa_\nu(\boldsymbol{x})\; I_\nu(\boldsymbol{x},\boldsymbol{n}) + j_\nu(\boldsymbol{x}). \quad (4)$$

The transport equation can be treated separately for the stellar and diffuse component because the radiation field is additive. However, numerical solutions for the diffuse part on the basis of the above analytic descriptions invokes serious difficulties because the nebular conditions are not known a priori, and because the coupling between radiation and matter is highly non-linear.

A first approach to solve for the radiation field is the so-called on-the-spot approximation where for the diffuse part the left-hand-side of eq. 4 is set to zero. An improvement represents the outward-only approximation. There the diffuse radiation is assumed to be emitted only into the outer hemisphere, and eq. 4 can be integrated radially-outward starting at the inner edge of the nebula. However, the latter approximation is no longer applicable when the diffuse contribution takes over the major role in the radiation field, as is for example the case in shadow zones. Neglecting the inward flow of diffuse radiation can cause substantial errors under such conditions. In the following paragraph we develop a a different numerical method to treat the radiative transfer adequately.

3. Photoionization modeling using Monte Carlo techniques

3.1. Basic ideas

The main principle of this approach consists of the local simulation of the individual processes of ionization and recombination. Therefore the radiation field is expressed in photon packets rather than in terms of intensity. Energy conservation is imposed naturally and verified by properly including and counting all input and output channels.

To start one considers a photoionized nebula in equilibrium. A representative number of photon packets is created at the position of the ionizing star inside the nebular shell. A packet of

energy ΔE_ν consists of a varying number n of photons depending on their uniform frequency ν according to

$$\Delta E_\nu = n\,\mathrm{h}\nu. \tag{5}$$

The reason for this choice is twofold. Firstly, a feasible and sufficient number of photon packets $N_{\rm ph}$ for computing the radiation field turns out to be around 10^5, far below realistic numbers of photons emitted by the source, ranging $\sim 10^{40}$phot/s. Secondly, the star's total luminosity L_* is evenly split up amongst the packets, so that the energy represented by one packet in the time interval Δt, the duration of the Monte Carlo experiment, is

$$\frac{L_*}{N_{\rm ph}} = \frac{\Delta E}{\Delta t}. \tag{6}$$

If such a packet gets absorbed and subsequently re-emitted at a different frequency, only the number of photons it contains will change. This feature of the Monte Carlo method provides the strict energy conservation at any one point in the nebula.

The photon energy realized in an individual packet is derived from the frequency distribution (i.e. the input spectrum) of the ionizing star (or a superposition of spectra in case of an ionizing cluster), so the probability for a frequency lying in the interval $(\nu, \nu + d\nu)$ is

$$p(\nu)\mathrm{d}\nu = \frac{F_\nu \mathrm{d}\nu}{\int_{\nu_{\rm H}}^{\nu_{\max}} F_\nu \mathrm{d}\nu'} = \frac{F_\nu \mathrm{d}\nu}{L_*/(4\pi R_*^2)}, \tag{7}$$

where F_ν denotes the stellar flux. Since stellar photons with energies below the H limit pass through the nebula without further interaction they have no net effect on the energy balance. The upper integration limit is truncated properly depending on the stellar spectrum. Each photon packet is now tracked on its way through the nebula while the series of events it suffers, the photon packet history, is stored. Once it has been turned into photons with a frequency below any ionization threshold, the packet escapes to infinity, and contributes to the observable spectrum. Once a set of photon packet histories is complete their contributions at a given position r and frequency ν are summed up in order to form the total mean intensity.

When a photon packet is emitted by the stellar source, it enters the nebula at the inner edge $R_{\rm in}$, specified in advance. Its direction of propagation is radially outward, perpendicular to the surface defined by a sphere with radius $R_{\rm in}$. There the photon packet is exposed to a finite optical depth given by

$$\tau_\nu(s) = \int_0^s \kappa_\nu \,\mathrm{d}s', \tag{8}$$

with the opacity $\kappa_\nu = \sum_i X_i a_\nu(X_i)$. The path length a photon packet traverses before it is absorbed is derived from the probability of absorption occurring at a distance $\leq s$ according to

$$P(s) = \int_0^s \mathrm{e}^{-\kappa_\nu s'} \kappa_\nu \mathrm{d}s';\ P(s) = 1 - \mathrm{e}^{-\kappa_\nu s} \text{ for const. } \kappa_\nu \tag{9}$$

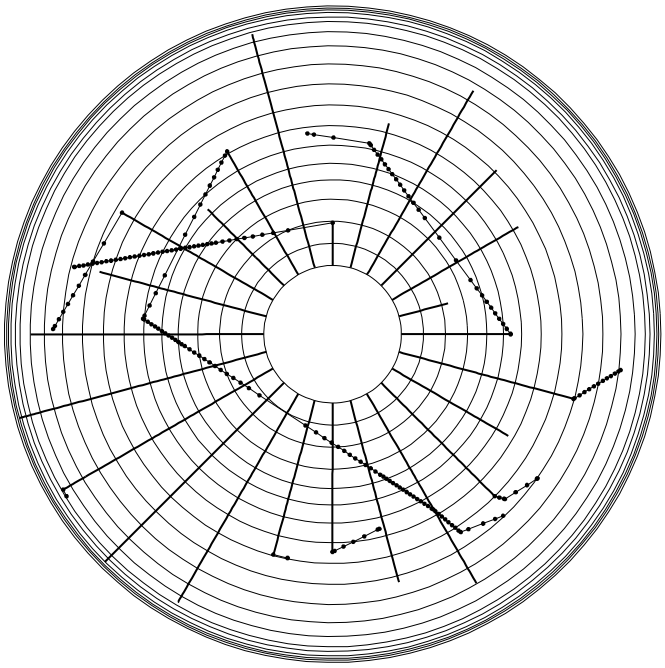

Fig. 1. The random walks for several photon packages starting at the inner nebular radius are plotted. Stellar photon packages are shown as thick lines, while diffuse packages passing reference positions are represented by filled dots (only every fifth radial grid surface is drawn). Once they have turned into non-ionizing packages, they are no longer tracked since they escape immediately.

$P(s)$ can be represented by a random number ξ, which is uniformly distributed in the interval $[0, 1]$. Given ξ, the path length s of a particular packet is found by inverting Eq. 9:

$$s = \frac{-\ln(1-\xi)}{\kappa_\nu}. \tag{10}$$

The generalization for a multiple phase medium requires a piecewise homogeneous representation of its components, as realized in any numerical discretization of a continuous quantity. The total path length $s_{\rm tot}$ covered in a composite medium where each component j with opacity $\kappa_\nu(j)$ contributes with s_j, then amounts to

$$s_{\rm tot} = \sum_{j=1}^{l-1} s_j - \left(\frac{\ln(1-\xi) + \sum_{j=1}^{l-1} \kappa_\nu\,(j)\, s_j}{\kappa_\nu\,(l)} \right). \tag{11}$$

After the absorption of a photon packet in a particular volume element (grid point), another packet is instantaneously emitted at the same position. The new direction into which it will propagate needs to be determined. Since absorption and re-emission are independent events and isotropic emission can be assumed, the direction cosines are distributed uniformly:

$\cos\theta = -1 + 2\xi$.

The angle θ is defined between the direction of propagation and the normal to the reference surface (e.g. a spherical surface centered on the photon source), and ξ is a newly created random

number. This assumption must be modified by the appropriate correlation between initial and final angle when anisotropic conditions, for example dust scattering, prevail.

In addition the photon packet is emitted with a new frequency, and the spectrum of the local emissivity has to be determined, complete as regarding continuum and line emission of any ion involved in order to fulfill energy conservation rigorously. The reprocessing of radiation is central to the Monte Carlo approach and will therefore be discussed separately below.

Having generated a new photon packet which is described by a (θ, ν) pair, the path length it travels until its next interaction is again found from Eq. 11. The packet's random walk is then continued until the outer radius of the nebula is exceeded and the photons escape. Sample photon packet histories for a 1D and spherical symmetric case are plotted in Fig. 1 together with the reference surfaces.

3.2. Calculation of mean intensity

The relation between specific intensity I_ν (using spherical coordinates r, θ) and corresponding photon energy E is provided by the definition of the specific intensity

$$\Delta E = I_\nu\,(r,\theta)\,\Delta A\,|\cos\theta|\,\Delta\nu\,\Delta\omega\,\Delta t, \tag{12}$$

with ΔA being the reference surface element, θ the polar and $\Delta\omega$ the solid angle. The mean intensity J_ν is derived from I_ν by summing over the full solid angle, i.e. calculating the zero order moment of I_ν according to

$$4\pi J_\nu\,(r) = \int_\Omega I_\nu\,(r,\theta)\,\mathrm{d}\omega = \frac{\Delta E}{\Delta t}\sum_{i=1}^{N_k}\frac{1}{|\cos\theta_i|}\frac{1}{\Delta A}\frac{1}{\Delta\nu} \tag{13}$$

by substituting $I_\nu \mathrm{d}\omega$ from Eq. 12. The sum is taken over all photon packets N_k with frequency in $(\nu, \nu+\Delta\nu)$, passing ΔA under an angle θ. The energy flow across ΔA, the flux F_ν, is then given by the first order moment of I_ν and expressed with the above as

$$\pi F_\nu = \int_\Omega I_\nu|\cos\theta|\mathrm{d}\omega = \frac{\Delta E}{\Delta t}N_k\frac{1}{\Delta A}\frac{1}{\Delta\nu}. \tag{14}$$

In order to establish a relation between the flux at frequency ν and the luminosity L_* of the ionizing star(s), the luminosity of a closed surface A at r, including the stellar source can be written as

$$L(r) = \sum_A\sum_\nu \pi F_\nu\,\Delta\nu\,\Delta A = \frac{\Delta E}{\Delta t}N_{\rm ph} \equiv L_* \tag{15}$$

Here the sums are over any photon packet crossing this surface or, equivalently, any photon emitted by the source in the time interval Δt. Because the nebula is assumed to be in quasi-static equilibrium, and because neither sinks nor sources of energy exist inside the gas, the luminosity (net energy flow) through a closed shell around the stellar source(s) is constant and equal to L_*. Although the (r, θ) coordinates suggest spherical symmetry, this approach is independent of the actual geometry chosen for the nebula. The only complication coming in for an arbitrary 2D geometry is the explicit determination of the path length s in a particular volume element.

3.3. Reprocessing of radiation

Following the absorption of a photon packet, the new frequency is derived by sampling the spectral energy distribution of the total local emissivity $j_\nu^{\rm tot}$. For the Monte Carlo model, the amount of energy released, e.g. in the optical, needs to be calculated in detail in order to satisfy the thermal energy balance implied. Therefore all major emission processes corresponding to possible energy channels have to be taken into account, in particular the complete non-ionizing nebular line and continuum emission. Although the latter leaves the nebula without further interaction it is necessary to properly incorporate this radiation, because it has its origin inside the nebula and appears on the energy budget. As a by-product the contents of these channels of non-ionizing radiation are the Monte Carlo simulated "observable spectrum" ready for comparison with observations or with spectra calculated from local conditions. The frequency range has to be chosen large enough to include the bulk of the energy emitted. In the following the individual contributions to the emissivity are discussed.

The H I recombination spectrum is composed of line and continuum radiation. The H I continuum can be divided into an ionizing part, the Lyman continuum, and a non-ionizing part, the continua from Balmer-, Paschen- and all higher series as well as the 2-photon continuum emitted in the transition $2^2S - 1^2S$ (Brown & Mathews 1970). The production rate of ionizing continuum photons in the higher series is negligible. The emissivity of the Lyman continuum is computed directly from Eq. 2. Recombination lines between the lower levels n=2 through 8 and upper levels n=3 through 15 are calculated for Case B according to Hummer & Storey (1987). In Case B the conversion of recombination lines connected to the ground state into lines of higher series is already taken into account, and the Lyman lines do not show up separately in the energy balance. However, one exception exists, namely the Lyman-α line. Because the line profiles are represented by δ-functions (i.e. no Doppler-shifts are considered), and other destruction mechanisms, dust for instance, are missing, all Lyman α photons eventually leave the nebula after emission and their contribution has to be added to the energy balance.

Presently we consider only singly ionized helium. Its treatment in general follows the one of the hydrogen spectrum explained above. For the non-ionizing contributions, the continuum emission follows Brown & Mathews (1970), while the recombination line strengths for frequencies below the H I limit are taken from Brocklehurst (1972). However, the line transitions connected to the 1^1S ground state of He I produce emission lines capable of ionizing H and low ionization stages of other elements. In detail the emission the He I Lyman lines for n=2 through 5 (Brocklehurst, 1972) and the intercombination lines with transitions $2^3S - 1^1S$ and $2^3P - 1^1S$ (Robbins 1968) are

calculated as a function of temperature. These lines are properly considered in the emission spectrum by adding their respective contributions to the corresponding frequency interval. The 2-photon continuum of the $2^1S - 1^1S$ transition (Drake et al. 1969) is correctly incorporated, contributing in part also to the diffuse ionizing radiation. Since the emission profiles of the He I lines (as well as any other line emission) are currently treated as δ-functions, the line opacity is assumed to be zero and line absorption is only due to the continuum opacity.

For the heavy elements, the free-bound continua for recombination into the ground state are calculated according to Eq. 2. The photoionization cross sections for sulfur are those of Chapman & Henry (1971), while the remaining values are taken from Henry (1970). Most of the ions are treated as 5-level atoms in order to derive the emissivities of the forbidden lines (eg. De Robertis et al. 1987). Due to incomplete atomic data, only a 2-level atom is used for Ne^+. The line emission of $\mathrm{C}^0, \mathrm{C}^{3+}, \mathrm{N}^{3+}, \mathrm{Ne}^0$, and S^0 is not included because the amount of energy deposited there is negligible.

The energy distribution of the resulting total emissivity follows from the summation over all contributions to a certain frequency interval $(\nu, \nu + \mathrm{d}\nu)$. Line emission with an energy below the H I limit is treated separately in order to get the line luminosities exactly. Together with the photons emitted in the lower free-bound continua they cannot cause further ionizations and escape from the nebula. The probability for converting an (either stellar or already processed) ionizing photon packet into a non-ionizing one is then given by the fraction of energy emitted in these channels

$$P_{\mathrm{esc}} = \frac{\sum_i j^{\mathrm{l}}_{X_i} + \int_0^{\nu_{\mathrm{H}}} j^{\mathrm{c}}_\nu \mathrm{d}\nu}{\sum_i j^{\mathrm{l}}_{X_i} + \sum_i j^{\mathrm{l}}_{\mathrm{He\,I}} + \int_0^{\nu_{\mathrm{He}^+}} j^{\mathrm{c}}_\nu \mathrm{d}\nu}. \quad (16)$$

The upper limit for the continuum radiation is justified by the (assumed) absence of a He^{2+} zone, which corresponds to a limitation in the ionizing source's T_{eff}, i.e. a negligible He^+-ionizing photon flux. Although the overall solution does not depend on the detailed choice of whether a line or a continuum packet is to emerge, the nebular line spectrum is eventually computed by making this decision and storing the information at this point.

If the decision was made for an ionizing packet, the new frequency is derived from the *probability density function* (PDF) for this radiation according to

$$p(\nu) = \frac{j^{\mathrm{c}}_\nu + j^{\mathrm{l}}_{\mathrm{He\,I}}}{\int_{\nu_{\mathrm{H}}}^{\nu_{\mathrm{He}^+}} (j^{\mathrm{c}}_\nu + j^{\mathrm{l}}_{\mathrm{He\,I}}) \mathrm{d}\nu'}, \quad (17)$$

where the He I resonance lines are added in the corresponding frequency bin.

The PDFs for ionizing and escaping photons at each grid point depend on the local T_{e}, n_{rme} and ionization structure. Physical parameters such as gas density or element abundance can be specified differently in every volume element. A simple but nevertheless challenging case is for example a spherically symmetric nebula with a non-monotonic density law. While several approximations are necessary in conventional numerical solution schemes (cf. Sect. 2), the present Monte Carlo technique does not require any particular assumptions about the physical structure and ensures a rigorous determination of the total radiation field.

At last, the scheme started with a preset nebula, local conditions eventually prescribed by using results from an analytic photoionization model or even just approximate values from the back of envelope calculations. Because of the rigorous local and global energy conservation, local conditions not in accord with a good solution will result in a net flow into or out of the volume element. Its spectral energy distribution can now be utilized to improve on the local conditions in a next iteration step.

Table 1. Parameters of the benchmark H II region. Elemental abundances are by number with respect to H.

$Q_{\mathrm{bb}}(\mathrm{H})$	$4.26\,10^{49}\mathrm{phot/s}$
	$= 1.25\,10^{39}\mathrm{erg/s}$
R_{in}	$3.0\,10^{18}\mathrm{cm}$
T_{eff}	40 000K
N_{H}	$100\ \mathrm{cm}^{-3}$
He	0.1
C	$2.2\,10^{-4}$
N	$4.0\,10^{-5}$
O	$3.3\,10^{-4}$
Ne	$5.0\,10^{-5}$
S	$9.0\,10^{-6}$

4. Application to homogeneous test case

4.1. Model H II region

The H II region considered here is assumed to be spherical symmetric with an ionizing star in its center emitting a blackbody spectrum. The nebula itself is treated in quasi-static equilibrium and radiation-bounded. The gas density distribution is homogeneous, and the elements H, He, C, N, O, Ne, and S are present. As is usual practice, trace elements such as Cl and Ar are not considered for the photoionization calculation. The detailed chemical composition together with remaining physical parameters are summarized in Table 1. All heavy ions are included in the calculation of the opacity, as well as most of their contributions to the cooling rate (cf. Sect. 3.3).

4.2. Iterative procedure

In order to start the random walks of the photon packets, the initial conditions (ionization structure, T_e) need to be specified: R_{Str} is estimated from L_*; for example an exponential distribution for the H and He ionization structure is imposed; T_{e} is set to $10000\mathrm{K}$. The actual choice of the initial set-up has no impact on the final result, but will strongly influence the number of iterations required for convergence.

After a discretization of the nebula into concentric shells, the frequency dependent total emissivity is calculated for each shell

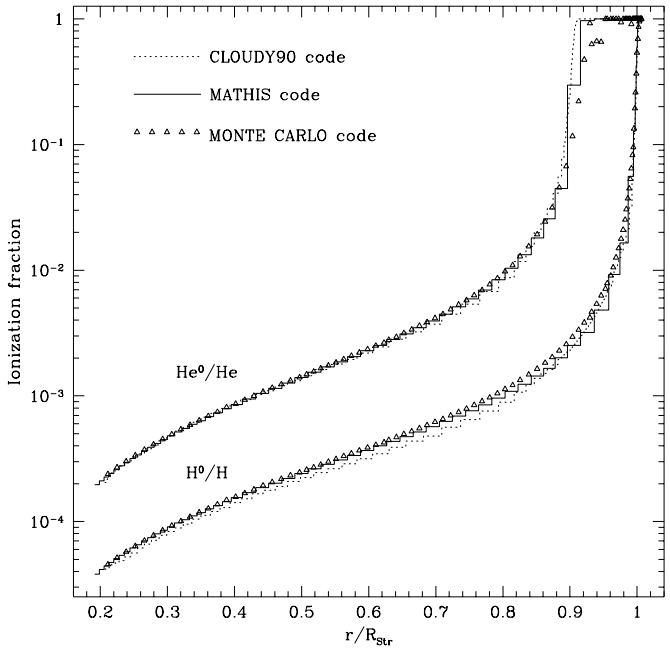

Fig. 2. Resulting ionization fraction of H and He for models using different radiative transfer methods. In the Monte Carlo code statistical fluctuations appear where the photon statistics decreases, e.g. at the $\mathrm{He}^+ - \mathrm{He}^0$ transition zone. Parameters for the nebula follow from Table 1.

to set up the PDFs which in turn determine the re-emission frequencies during the simulation. The PDF for the stellar packets is derived from the input spectrum and is computed only once at the beginning. Then the photon histories for the number of packets chosen are collected as described earlier and the stellar and diffuse mean intensity J_ν is summed up according to eq. 13. To update the initial model, the ionization balance is solved simultaneously with the thermal balance providing the new ionization and temperature structure. The above sequence is iterated until convergence is achieved. The criterion might be for example an upper limit of the difference between the H ionization structures of subsequent iterations.

4.3. Variation of the outer radius

Since the estimated R_{Str} can differ significantly from the final solution, the outer radius of the model must be allowed to adjust to the changing nebular conditions. Thus radial points are added at the outer edge as necessary for an extension of the ionized volume. In addition, radial grid points are inserted or removed as required in order to maintain a minimum photon flux through each shell, which enables a meaningful determination of, e.g., a non-zero heating rate. This adjustment also prevents packets from getting trapped in a shell which has an optical depth too large to be passed with a reasonable probability. While the radial grid points are discrete quantities (each belonging to one set of T_{e}, ion abundances, and radiation field) the photon path length s is a continuous one. The shells' geometric midpoints serve as reference surfaces where the traversing packets are counted.

4.4. Calculation of line strengths

The final model obtained has to be compared either with other models or with observations of real nebulae. This is achieved by calculating the surface brightness of various emission lines. The result of the Monte Carlo simulation provides two methods to determine these line intensities.

To calculate the luminosity of the nebula in a given line the number of photon packets $N_{\mathrm{line}}(r_i)$ are summed over the total number of shells $i_{\max}$, and directly yield the amount of energy emitted in that line according to

$$L_{\mathrm{line}} = \frac{\Delta E}{\Delta t} \sum_{i=1}^{i_{\max}} N_{\mathrm{line}}(r_i), \tag{18}$$

where $\frac{\Delta E}{\Delta t}$ is given by Eq. 6.

An alternative way, the only one available to analytic models, is the integration of the line emissivity over the volume, since the local values of T_{e} and of the ionic abundances are a natural result of the final model.

For Monte Carlo simulations both methods yield consistent results, provided the final iteration is run with enough packets to yield good statistics for even the faintest line considered.

5. Results and comparison with analytical models

The results from several established photoionization models applying analytical techniques are now compared with those supplied by the Monte Carlo (MC) method. Therefore the parameters for an H II region as specified above are chosen as the uniform input set. Both radial dependent and integrated quantities are looked at to check the overall agreement of the solutions.

The H and He ionization structure is a major characteristic of a nebula and provides a general check of the MC code since a consensus exists in the atomic data used. The results for an outward-only model (CLOUDY90), an outward-inward iteration scheme (Mathis 1976), and the MC code are shown in Fig. 2. There is very good agreement for both these ions among all 3 methods (see figure caption).

The resulting line ratios and the absolute quantities $L(\mathrm{H}_\beta)$ and R_{Str} for the H II region specified in Table 1 are listed in Table 2, together with the results of other photoionization codes as presented at a workshop held at Lexington in 1994 (cf. Ferland et al. 1995). In principle each code should convert the same number of ionizing photons into the same luminosity $L(\mathrm{H}_\beta)$ (viz. R_{Str}). The subtle differences are due to the way in which the ionizing radiation is redistributed (branching ratios, lines to be considered, He model atom). However, the crucial quantities, namely the total number of H and He ionizing photons have been checked very carefully.

Variations in the relative line strengths as for example in [S II]λ6720 are clear hints to different atomic data bases and/or changes of atomic parameters over the last decades. However, the MC model results of all integral quantities available for comparison lie well within the scatter defined by the classical

Table 2. Line intensities for the H II region characterized by Table 1 with respect to H_β, the latter given in absolute units. Multiplets are marked by a + following the wavelength. T_e at the inner nebular edge and weighted by H^+ are listed, the mean ionization fraction of H to He, and R_{Str} in cm.

		Mappings[a]	Cloudy[b]	Harrington[c]	Rubin[d]	This work
$L(H_\beta)$	10^{37}erg/s	1.96	2.06	2.04	2.05	1.78
HeI	5876	0.125	0.109	0.119		0.123
CII	2326+	0.07	0.19	0.17	0.18	0.17
CIII]	1909+	0.050	0.059	0.059	0.076	0.066
[NII]	122 μ	0.032	0.033		0.031	0.034
[NII]	6584+	0.61	0.88	0.74	0.73	0.78
[NIII]	57μ	0.16	0.27	0.29	0.30	0.32
[OII]	3727+	1.50	2.19	2.14	2.26	2.26
[OIII]	51.8 μ	1.10	1.04	1.11	1.08	1.13
[OIII]	88.4 μ	1.30	1.07	1.28	1.26	1.31
[OIII]	5007+	2.30	1.93	1.96	2.10	2.11
[NeII]	12.8μ	0.26	0.23	0.19	0.20	0.27
[NeIII]	15.5μ	0.37	0.43	0.43	0.42	0.38
[NeIII]	3869+	0.085	0.103	0.086	0.087	0.077
[SII]	6720+	0.24	0.23	0.16	0.13	0.15
[SIII]	18.7μ	0.56	0.48	0.56	0.58	0.61
[SIII]	34μ	0.91	0.82	0.89	0.94	0.97
[SIII]	9532+	1.16	1.27	1.23	1.30	1.38
[SIV]	10.5μ	0.22	0.37	0.42	0.33	0.37
$T_{\rm inneredge}$	K	7630	7815	7741	7399	7452
$T(H^+)$	K	7880	8064	8047	8087	8060
$\langle He^+\rangle/\langle H^+\rangle$			0.71	0.77	0.83	0.78
$R_{\rm Str}$	10^{19}cm	1.43	1.46	1.46	1.46	1.42

[a] Binette et al., 1993a, 1993b
[b] Ferland et al., 1994
[c] Harrington et al., 1982
[d] Rubin, 1985

codes. Therefore all further analysis done via diagnostic diagrams or direct spectral modeling can be carried out with the same accuracy as defined by the classical codes.

6. Summary

The key problem in modeling inhomogeneous and non-isotropic media is the correct treatment of the radiation transport. We explored the Monte Carlo technique as a proven means to handle complex radiation transport problems. We have shown that its application to photoionized nebulae allows one to treat the radiation transport irrespective of the actual gas distribution or nebular geometry.

Using the Monte Carlo methodology we then developed a 1D photoionization program and compared the results for a homogeneous nebula with those from several classical photoionization codes in general use. As expected, the ionization structure and mean temperatures, as well as emission line ratios agree very well. The Monte Carlo technique, the method of choice from theoretical considerations, therefore proves to be ready for application to the more interesting non-homogeneous and more-dimensional cases.

Acknowledgements. S.R. Och gratefully acknowledges support by an ESO studentship. The referee J.S. Mathis provided us with challenging questions on the internal consistency of the method.

References

Abbott, D.C., Lucy, L.B. 1985, ApJ, 288, 679
Binette, L., Wang, J.,Villar-Martin, M., Martin, P.G.,Magris, C.G. 1993a, ApJ, 414, 535
Binette, L., Wang, J., Zuo, L., Magris, C.G. 1993b, AJ, 105, 797
Brown, R.L., Mathews, W.G. 1970, ApJ, 160, 939
Brocklehurst, M. 1972, MNRAS, 157, 211
Chapman, R.D., Henry, R.J.W. 1971, ApJ, 168, 169
De Robertis, M.M., Dufour, R.J., Hunt, R.W. 1987, J. R. Astron. Soc. Canada, 81, 195
Drake, G.W.F., Victor, G.A., Dalgarno, A. 1969, Phys.Rev., 180, 25
Ferland, G.J., 1994, *Hazy*, University of Kentucky Department of Physics and Astronomy Internal Report

Ferland, G., Binette, M., Contini, M.,Harrington, J., Kallmann, T., Netzer, H., Pequignot, D., Raymond, J., Rubin, R., Shields, G., Sutherland, R., Viegas, S., 1995, in: *The analysis of emission lines*, STScI Symposium Series 8, eds. R.E. Williams, M. Livio, Cambridge University Press, pp.83-96
Garnett, D.R. 1990, ApJ, 363, 142
Harrington, J.P., Seaton, M.J., Adams, S., Lutz, J.H. 1982, MNRAS, 199, 517
Henry, R.J.W. 1970, ApJ, 161, 1153
Hester, J.J., Gilmozzi, R., O'Dell, C.R., Faber, S.M., Campbell, B., Code, A., Currie, D.G., Danielson, G.E., Ewald, S.P., Groth, E.J., Holtzman, J.A., Kelsall, T., Lauer, T.R., Light, R.M., Lynds, R., O'Neil, E.J., Jr., Shaya, E.J., Westphal, J.A. 1991, ApJ, 369, L75
Hummer, D.G., Storey, P.J. 1987, MNRAS, 224, 801
Lucy, L.B., Abbott, D.C. 1993, ApJ, 405, 738
Mathis, J.S. 1976, ApJ, 207, 442
Mathis, J.S. 1982, ApJ, 261, 195
Mathis, J.S. 1985, ApJ, 291, 247
Mathis, J.S. 1995, Rev.Mex.A.A. *(Serie de Conferencias)*, 3, 207
Mathis, J.S., Rosa, M.R. 1991, A&A, 245, 625
Robbins, R.R 1968, ApJ, 151, 497
Rubin, R.H. 1985, ApJS, 57, 349
Strömgren, B. 1939, ApJ, 89, 526